Plasmons and the quantum limit in semiconductor wires

Florent Perez* and Bernard Jusserand
France Telecom/CNET/Laboratoire de Bagneux, Boîte Postale 107, 92225 Bagneux Cedex, France

Bernard Etienne
CNRS/L2M, Boîte Postale 107, 92225 Bagneux Cedex, France

(Received 29 June 1998; revised manuscript received 7 June 1999)

We report on the observation by Raman scattering of one-dimensional plasmons in deep-etched wires with lateral sizes w down to 30 nm. We determine the dispersion of these collective excitations down to 45 nm, well beyond the transition to a single one-dimensional subband occupancy ($w \sim 60$ nm), and demonstrate that they can be well described both within the random-phase approximation and the Lüttinger liquid theory. In thinner wires, the Raman spectra reduce to a single undispersive low-energy line which we attribute to a plasmon localized by longitudinal disorder in the external potential. [S0163-1829(99)01140-6]

One-dimensional (1D) confinement of electrons in semiconductor quantum wires is expected to provide unique electrical properties such as high electron mobilities,[1] quantized conductances,[2] or improved transconductance in field-effect transistors.[3] The observation of these specific properties relies on the fabrication of very narrow wires, with only one subband occupied and with very low disorder. At the present time, cleaved edge overgrowth[4] and organized growth on vicinal surfaces[5] have been demonstrated to provide very low lateral dimensions, of the order of 10 to 20 nanometers, with reduced disorder. On the other hand, deep reactive ion etching (RIE) provides the greatest flexibility to achieve strong confinement in arbitrary geometries but usually suffers from limitations in the lowest size easily realizable and from the presence of a high density of etching defects created on the lateral sidewalls of the quantum wire. We have shown previously from the observation by electronic Raman scattering of narrow lines related to the laterally confined plasmons that an electrochemical oxidation after the RIE process leads to high-quality one-dimensional electron gases (1DEG's) with a lateral size below 100 nm and a very abrupt equilibrium density distribution.[6,7]

On the other hand, there is a single report[8] of Raman scattering by intrasubband and intersubband plasmons in narrow wires, namely a shallow etched wire with two subbands occupied. Since this report, the validity of the random-phase approximation[9] (RPA), even when including exchange and correlation corrections,[10] to describe a 1DEG has been long debated in competition with the Lüttinger liquid behavior predicted at 1D by more recent theories.[11] Experimental signatures of a Lüttinger liquid behavior on semiconductor wires is presently actively investigated.[12] In this paper, we report on the observation of dispersive one-dimensional plasmons in deep-etched wires with lateral sizes down to 45 nm, i.e., significantly below the quantum limit where only one subband is occupied. We analyze these results in terms of different quantum descriptions of the plasmon energies. Below 45 nm, the dispersive plasmon disappears while a new nondispersive electronic excitation emerges. We attribute this excitation, observed down to the lowest fabricated size (30 nm), to the localization of the 1D plasmon by the potential fluctuations.

Starting from a 18-nm-thick modulation-doped $GaAs/Ga_{0.7}Al_{0.3}As$ single quantum well with a two-dimensional density $n_S = 5 \times 10^{11}\,cm^{-2}$ and a mobility of $7.0 \times 10^5\,cm^2\,V^{-1}\,s^{-1}$ at 4 K, the quantum wires have been prepared by reactive ion etching with an etched depth of 300 nm, much deeper than the quantum well, located at 150 nm below the surface. The patterns have been defined by electronic nanolithography. The damaged part of the lateral surfaces of the wires have been passivated by anodic oxidation.[13] This additional process results in the formation of an isotropic oxide layer with a thickness of 40 nm. The oxidation reduces by 80 nm the lateral size of the active region and limits the electron trapping in the damaged part. We have realized wires with different nominal widths w_{nom} (defined as the etched width corrected from the oxide thickness) ranging from 30 to 60 nm by 5-nm steps. For the narrow wires considered in this work, the resolution of scanning electron microscopy (SEM) images on desoxidized wires is hardly sufficient to measure this width with an accuracy better than 5 nm but allows us to observe a clear regular decrease in the nominal size following the coded patterns. On the other hand, size fluctuations along the wires have been estimated independently from luminescence on undoped wires and from the line broadening of plasmons in doped wires, consistently giving 5 nm in both cases. For these reasons we will only use w_{nom} in this paper to label the different wire arrays but never to quantitatively support any theoretical analysis of the data. As shown below, the systematic decrease of the intraband plasmon energy when reducing the width is, in our opinion, a good indication that our size control is better than 5 nm.

In this paper we present Raman scattering results in arrays of quantum wires of nominal width $30\,nm < w_{nom} < 60\,nm$. Quasibackscattering experiments have been performed at 2 K with an incident laser energy ($\sim$1.59 eV) in strong resonance with interband transitions associated with the second conduction subband of the GaAs single quantum well and an incident power density tuned between 1 and 5 W/mm.[2] Plasmon frequencies were found to be independent of the illumination power. The plasmon wave vector transferred to the 1DEG along the wire axis is varied according to the follow-

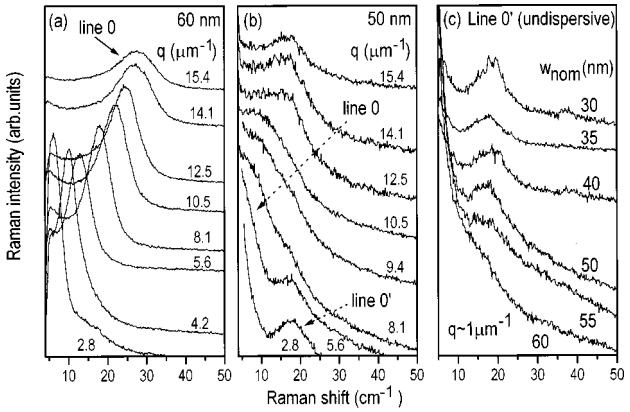

FIG. 1. Raman spectra measured in parallel polarization. (a) and (b) For two different wire widths $w_{nm}=60$ nm (a) and 50 nm (b) at various wave vectors and (c) for different wire widths at $q \sim 1.0\ \mu\mathrm{m}^{-1}$.

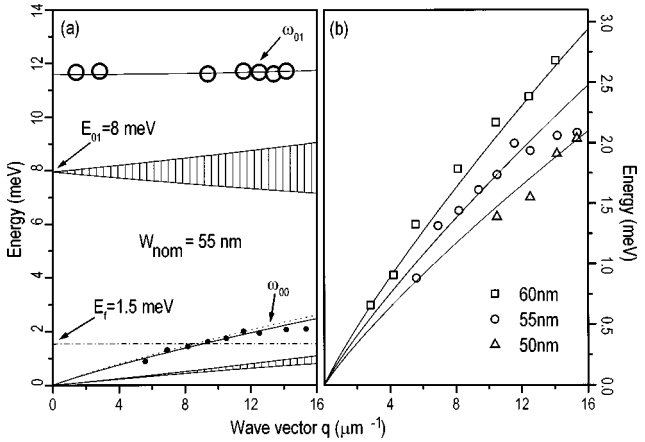

FIG. 2. Intra- and interband plasmons dispersions. (a) Extraction of the Fermi level E_f and the intersubband spacing E_{01} for the 55-nm wire by fitting dispersions of intraband (solid circle) and interband (open circle) modes. This correspond to a fitted width $w_{elec}=47\pm1.3$ nm and a one-dimensional density $n_1=(3.6\pm0.3)\times10^5\ \mathrm{cm}^{-1}$. Diameter of the circles equals the width at mid-height of the Raman lines. The Lüttinger result calculated for the same parameter is also shown (dotted line). (b) Intraband plasmons (line 0) for different wires. Experimental dispersions have been fitted with the RPA model presented in the text. The densities obtained are, respectively, with decreasing width: $n_1=4.5$, 3.6, and $2.4\times10^5\ \mathrm{cm}^{-1}$.

ing relation: $q=(2\pi/\lambda)(\sin\theta_i+\sin\theta_s)\cos\varphi$, where λ is the incident wavelength, θ_i and θ_S the incidence angle of the incoming and scattered light, respectively, and φ the angle between the plane of incidence and the wire axis. When φ vanishes, the plasmons with even and odd parities with respect to the mirror plane along the wire axis are observed in parallel and crossed polarization, respectively.[14] In parallel polarization, the low-energy Raman spectra on wires with $w_{nom}\geqslant45$ nm are dominated by a dispersive line (line 0), as illustrated in Figs. 1(a) and 1(b) for $w_{nom}=60$ and 50 nm, respectively. Below 45 nm, the dispersive mode is no longer observed and the Raman spectra are dominated by an undispersive Raman line (line $0'$). This line is also present in the thicker wires but is only resolved from the dispersive line at wave vectors $q\leqslant2\ \mu\mathrm{m}^{-1}$. As illustrated in Fig. 1(c), the frequency of line $0'$ slightly increases with decreasing lateral size. In crossed polarization, a new line (line 1, not shown in Fig. 1) appears at higher energy for $w_{nom}\geqslant55$ nm, with a negligible dispersion as compared to the line broadening, whereas both lines 0 and $0'$ disappear in this configuration. Below this lateral size, no significant contribution is observed in crossed configuration. According to the parity selection rules for one-dimensional plasmons in etched wires,[14] we attribute line 1 to an odd-parity plasmon, while lines 0 and $0'$, observed in parallel polarization, are related to the lowest-energy even-parity plasmon.

We have analyzed the electronic excitations in our wires within the RPA quantum model.[15] In a previous study[7] on thicker wires, we have determined the external potential acting on the free electrons. This potential is almost parabolic and the total potential including electron-electron interaction becomes quasirectangular. We have thus used eigenfunctions of a w_{elec} wide rectangular potential within the quantum model developed in this work. Through this model we have extracted from the plasmon dispersions the respective position of the Fermi level E_f and the intersubband spacing E_{01} (between the first and the second 1D confined levels) and we have determined whether the quantum limit, where only the first subband contains free electrons, is achieved. In the RPA description, an even (respectively, odd) plasmon mode results from the coupling through the Coulomb interaction of all single-particle excitations (SPE) between occupied and empty states of two one-dimensional subbands with the same parity (respectively, different parities). For an electron gas with one or two occupied subbands, as in the range of lateral sizes and densities corresponding to our experiments, it is possible to label the plasmon modes with the index of transition which contributes the most to the plasmon state, say, the SPE whose energy is the nearest from the considered plasmon mode. The depolarization shift corresponds to the difference between the plasmon energy ω_{nm} and the associated single-particle transition energy between subbands n and m: SPE_{nm}. One can thus unambiguously assign line 1 to ω_{01} and line 0 to ω_{00}. Based on these assignments, we have adjusted the wire thickness w_{elec} and the one-dimensional density n_1 on the measured dispersion curves of line 0 and line 1 for $w_{nom}=60$ and 55 nm. Only the result for the 55-nm wire is shown Fig. 2(a) as there is no qualitative change in the dispersions between the 60- and 55-nm wires. We find, respectively, for the 60- and the 55-nm wires: $E_{01}=8.0\pm0.4$ meV, $E_f=2.7\pm0.3$ meV and $E_{01}=8.0\pm0.4$ meV, $E_f=1.5\pm0.3$ meV, corresponding for the last one to a potential width $w_{elec}=47\pm1.3$ nm and a one-dimensional density $n_1=(3.6\pm0.3)\times10^5\ \mathrm{cm}^{-1}$. The fitted width is in a very good agreement with the nominal one. Concerning the density, the value is 20% of the total remote density given by $n_s\times w_{nom}=2.7\times10^6\ \mathrm{cm}^{-1}$, because the etching modifies the equilibrium distribution between electrons of the donor sheet and electrons from the gas. Remaining electrons (80% of the remote density) are probably trapped in the surface states introduced by the etching and do not contribute to the plasmon energy. A detailed Schrödinger-Poisson model[3] would be necessary to quantitavely support this assessment but this is out of the scope of this paper. As a result from the fit, both wires are found in the quantum limit in the frame of the RPA. However, according to more recent theories,[10] one

knows that exchange and correlation effects, which are not taken into account in the precedent RPA model, are very strong in one dimension: for a RPA parameter $r_s=4$ ($r_s=1/2n_1a^*$, where a^* is the electron Bohr radius in GaAs and $a^*=10\,\mathrm{nm}$), the exchange effect reduces the intraband plasmon energy by 30% from its RPA value.[10] In our samples, $r_s=1-2$, giving a lower exchange correction. In the absence of numerical calculations available for our situation, we will consider this correction as an additional incertitude added to the experimental incertitude. We try to fit again the experimental dispersion with respect to w_{elec} and n_1 according to the following relations:

$$\omega_{00}^{RPA}(1-\varepsilon_{00}^{exch})=\omega_{00}^{expt},$$

$$\omega_{01}^{RPA}(1-\varepsilon_{01}^{exch})=\omega_{01}^{expt},$$

where ε_{0i}^{exch} is the exchange correction for the intraband and interband plasmon. In the absence of available data for the exchange correction on the intersubband plasmon energy, we assume $\varepsilon_{00}^{exch}=\varepsilon_{01}^{exch}=30\%$ and we find for the 60-nm wire: $E_{01}=9.54\,\mathrm{meV}$ and $E_f=9.55\,\mathrm{meV}$. There is a slight occupation of the second subband: $d_1/(d_0+d_1)=3\%$, where d_i is the electron density in the subband i. This wire is no longer in the quantum limit when a very large exchange interaction is taken into account. For the 55-nm wire, we have considered the extreme case where the exchange strongly modifies the intraband plasmon energy but leaves unchanged the interband plasmon: $\varepsilon_{00}^{exch}=30\%$, $\varepsilon_{01}^{exch}=0\%$. We find $E_{01}=6.2\pm0.4\,\mathrm{meV}$, $E_f=5.0\pm0.3\,\mathrm{meV}$ and this wire is still in the quantum limit. A stronger exchange correction on the intersubband plasmon energy would increase the intersubband spacing and then reinforce our conclusion. For wires thinner than 55 nm, we cannot determine the electrical width w_{elec} due to the lack of clear line 1 in the corresponding Raman spectra. Nevertheless, we have used the remarkable feature that the ω_{00} dispersion weakly depends on the exact potential shape [see Fig. 3(a)], i.e., on w_{elec}, but mainly on the density n_1, to extract a good estimation of this quantity for $w_{nom}=50\,\mathrm{nm}$ [see Fig. 2(b)]. n_1 decreases regularly with the size between 60 and 45 nm, the latter being very close to the critical width where the free-electron density vanishes. Below this dimension, all remaining electrons become localized.

Based on these determinations, let us now analyze the experimental dispersion of the fundamental plasmon. We have added in Fig. 2(a) the dispersion calculated for the same density $n_1=3.6\times10^5\,\mathrm{cm}^{-1}$ and the same potential width $w_{elec}=47\,\mathrm{nm}$ within the Lüttinger model[11]

$$\omega(q)=\nu_f q\left[\left(1+\frac{g_1}{h\nu_f}\right)\left(1-\frac{g_1}{h\nu_f}+\frac{1}{h\nu_f}\frac{2e^2}{\pi\varepsilon}V(qw_{elec})\right)\right],$$

where ν_f is the Fermi velocity, e the electron charge, ε the dielectric constant of GaAs, g_1 a backscattering matrix element (the best fit is obtained for $g_1=0$), V is the Coulomb potential averaged over the wire section given by

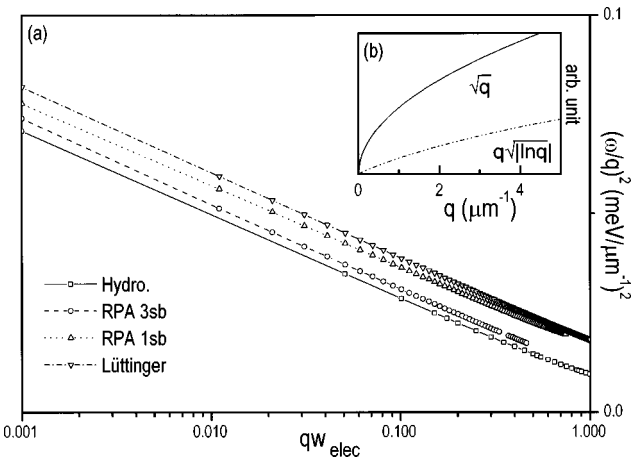

FIG. 3. One-dimensional plasmon versus one-dimensional electron gas. (a) Demonstration of the $q|\ln(q)|^{1/2}$ behavior followed by the three models: Hydrodynamic, RPA (one and three subbands occupied), and Lüttinger at small wave vector. All dispersions are calculated with the same density $n_1=3.6\times10^5\,\mathrm{cm}^{-1}$ and the same potential width $w_{elec}=47\,\mathrm{nm}$, except RPA with three subbands (RPA 3 sb) which is calculated with $w_{elec}=400\,\mathrm{nm}$. (b) Qualitative comparison between dispersions of a 2DEG intraband plasmon ($\sqrt{q}$) and a one-dimensional plasmon ($q|\ln(q)|^{1/2}$).

$$V(qw_{elec})=\left(\frac{2}{w_{elec}}\right)^2\int_{w_{elec}/2}^{w_{elec}/2}dx\int_{w_{elec}/2}^{w_{elec}/2}dx'\times K_0(q|x-x'|)\cos^2\left(\frac{\pi x}{w_{elec}}\right)\cos^2\left(\frac{\pi x'}{w_{elec}}\right).$$

Apart from a little correction originating from screening due to higher subbands (which is taken into account in the RPA but not in the Lüttinger model), the Lüttinger dispersion follows exactly the RPA one. According to the well-known argument that the RPA approach breaks down at 1D because of the singular behavior of the free-electron polarizability function at $2k_f$ (k_f is the Fermi wave vector), this comparison shows that the RPA remains valid as far as we consider wave vectors q well below the $2k_f$ value. This is the case for experimental dispersions involved here ($2k_f\sim100\,\mu\mathrm{m}^{-1}$).

Moreover, there is no specific behavior of the single subband occupancy character (in agreement with the results on the 60- and 55-nm wires) as there is no qualitative change between the Lüttinger dispersion ($g_1=0$) and RPA, dispersions with a growing number of occupied subbands. All dispersions of the one-dimensional plasmon behave in the long-wavelength limit like $n_1\times q|\ln(q)|^{1/2}$. This point is shown in Fig. 3(a) where we have plotted $(\omega/q)^2$ as a function of $\ln q$ for dispersions calculated with the same density but with different models: the RPA with one and three occupied subbands, the Lüttinger model, and the hydrodynamic model.[16] All dispersions are linear for small qw_{elec}. The slope is proportional to n_1^2 and is nearly the same depending on assumptions of the considered model. As shown in Fig. 3(b), this behavior qualitatively differs from a 2DEG plasmon with a square-root behavior and is a specific character of a quasi-one-dimensional intraband plasmon but not necessarily of a strictly one-dimensional electron gas.

Below 45 nm, the dispersive plasmon is no longer observed and we attribute the nondispersive line $0'$ to a one-

dimensional plasmon localized by potential fluctuations. The value of its energy excludes ($\sim$15 cm^{-1}) laterally confined acoustical phonons, whose energy would be around 1 cm^{-1} for this width of confinement. A first contribution to potential fluctuations reflects the lateral size fluctuations due to process limitations. Such fluctuations ($+-5$ nm) explains the broadening of line 1 with decreasing size and its nonobservation in the thinnest wires. This type of fluctuation, however, has a small influence on the 1D intrasubband plasmon, which is weakly sensitive to the exact shape of the potential. Moreover, the corresponding charge oscillations have a very long coherence length along the wire axis, as we showed previously in etched wires with an intentional periodic modulation of the lateral size:[17] they remain extended, whereas the higher energy plasmons are confined in the thickest parts of the wire. We thus must consider other sources of disorder to explain the plasmon localization in very narrow wires and the statistical distribution of Si donors in the remote doping layer is a good candidate to induce fluctuations of the confinement potential. As shown previously,[18] the effect of these fluctuations increases when the electron density decreases, which is likely to qualitatively explain our observations. Nevertheless, split gate structures have been considered in Ref. 18 where the external potential of donors does not depend on the wire width. This is not the case in deep-etched wires and stronger fluctuations due to donor distribution are likely to appear, as well as be evaluated by a detailed model of the real confining potential actually under development.

In conclusion, we have observed extended 1D plasmons in very narrow deep-etched wires and well reproduced their dispersion within a simple quantum model. While the higher plasmon branches are significantly broadened by lateral size fluctuations and become undetectable below 55 nm, the fundamental 1D plasmon remains extended at significantly smaller sizes and we attribute its final disappearance around 40 nm to potential fluctuations. We demonstrate that the measured plasmon dispersions can be well reproduced both within Fermi and Lüttinger liquid theories: in this range of lateral width and densities both theories predict identical plasmon dispersions for wave vectors small compared to $2k_f$. Deep etching allows us to realize 1D electron gases with small disorder. Limited improvement of the technological process should allow us to further reduce the density and the size and to evidence exchange and correlations corrections which behave differently in the Fermi and Lüttinger models.

*Present address: Laboratoire de Physique de la Matière Condensée, CNRS, UMR 5830, Complexe Scientifique de Rangueil, 31077 Toulouse cedex 04, France.

[1] H. Sakaki, Jpn. J. Appl. Phys. **19**, L735 (1980).

[2] D. A. Wharam, T. J. Thornton, R. Newbury, M. Pepper, H. Ahmed, J. E. F. Frost, D. G. Hasko, D. C. Peacok, D. A. Ritchie, and G. A. C. Jones, J. Phys. C **21**, L209 (1988); B. J. van Wees, H. van Houten, C. W. J. Beenaker, J. G. Williamson, L. P. Kouwenhoven, D. van der Marel, and C. T. Foxon, Phys. Rev. Lett. **60**, 848 (1988).

[3] S. Bollaert, P. Legris, E. Delos, A. Cappy, P. Debray, and J. Blanchet, IEEE Electron Device Lett. **41**, 1716 (1994).

[4] L. N. Pfeiffer, K. W. West, H. L. Störmer, J. P. Eisenstein, K. W. Baldwin, D. Gershoni, and J. Spector, Appl. Phys. Lett. **56**, 1697 (1990); W. Wegscheider, L. N. Pfeiffer, M. N. Dignam, A. Pinczuk, K. W. West, S. L. McCall, and R. Hull, Phys. Rev. Lett. **71**, 4071 (1993).

[5] B. Etienne, F. Laruelle, J. Bloch, L. Sfaxi, and F. Lelarge, J. Cryst. Growth **150**, 366 (1995).

[6] C. Dahl, B. Jusserand, and B. Etienne, Solid-State Electron. **40**, 261 (1996).

[7] F. Perez, S. Zanier, S. Hameau, B. Jusserand, Y. Guldner, A. Cavanna, L. Ferlazzo-Manin, and B. Etienne, Appl. Phys. Lett. **72**, 1368 (1998).

[8] A. R. Goni, A. Pinczuk, J. S. Weiner, J. M. Calleja, B. S. Dennis, L. N. Pfeiffer, and K. W. West, Phys. Rev. Lett. **67**, 3298 (1991).

[9] S. Das Sarma and E. H. Wang, Phys. Rev. B **54**, 1936 (1996).

[10] L. Calmels and A. Gold, Phys. Rev. B **52**, 10 841 (1998).

[11] H. Schultz, Phys. Rev. Lett. **71**, 1864 (1993); M. Sassetti and B. Kramer, *ibid.* **80**, 1485 (1998).

[12] S. Tarucha, T. Honda, and T. Saku, Solid State Commun. **94**, 413 (1995); A. Yacoby, H. L. Störmer, N. S. Wingreen, L. N. Pfeiffer, K. W. Baldwin, and K. W. West, Phys. Rev. Lett. **77**, 4612 (1996).

[13] J. Y. Marzin, A. Izrael, and L. Birotheau, Solid-State Electron. **37**, 1091 (1994).

[14] C. Dahl, B. Jusserand, and B. Etienne, Phys. Rev. B **51**, 17 211 (1995).

[15] L. Wendler and R. Haupt, Phys. Rev. B **52**, 9031 (1995).

[16] G. Eliasson, J. W. Wu, P. Hawrylak, and J. J. Quinn, Solid State Commun. **60**, 41 (1986).

[17] F. Perez, B. Jusserand, C. Dahl, M. Filoche, L. Ferlazzo-Manin, and B. Etienne, Phys. Rev. B **54**, R11 098 (1996).

[18] J. A. Nixon and J. H. Davies, Phys. Rev. B **41**, 7929 (1990).